Liquid Crystals

Publication details, including instructions for authors and subscription information:
http://www.informaworld.com/smpp/title~content=t713926090

Structural study of the aggregates formed by the dinucleoside phosphate G2 in aqueous solution

Lia Q. Amaral[a]; Rosangela Itri[a]; Paolo Mariani[b]; Ruggero Micheletto[b]
[a] Instituto de Fisica, Universidade de São Paulo, Brazil [b] Istituto di Fisica Medica, Università di Ancona, Ancona, Italy

To cite this Article Amaral, Lia Q. , Itri, Rosangela , Mariani, Paolo and Micheletto, Ruggero(1992) 'Structural study of the aggregates formed by the dinucleoside phosphate G2 in aqueous solution', Liquid Crystals, 12: 6, 913 — 919

To link to this Article: DOI: 10.1080/02678299208032807

URL: http://dx.doi.org/10.1080/02678299208032807

LIQUID CRYSTALS, 1992, VOL. 12, NO. 6, 913–919

Structural study of the aggregates formed by the dinucleoside phosphate G2 in aqueous solution

by LIA Q. AMARAL* and ROSANGELA ITRI
Instituto de Fisica, Universidade de São Paulo, Caixa Postal
20516, São Paulo, S.P., CEP 01498, Brazil

PAOLO MARIANI and RUGGERO MICHELETTO
Istituto di Fisica Medica, Università di Ancona,
Monte d'Ago, I-60131, Ancona, Italy

(*Received 20 February 1992; accepted 17 June 1992*)

X-ray diffraction results in magnetically oriented samples of aqueous solutions of the sodium salt of the dinucleoside phosphate G2 in the cholesteric N* phase are presented. The symmetry of the diffraction confirms a model of stacking of tetrameric disks forming cylindrical aggregates in the N* phase. A weak band at 7 Å not previously observed gives further information on the inner structure of the cylindrical aggregates. Analysis of the diffraction peak position in low angle evidences a change in functional behaviour of the distance a between cylinder axes as a function of the volume concentration c_v of G2. In the H phase, $a \propto c_v^{-1/2}$ as it should for infinite cylinders; in the N* phase, $a \propto c_v^{-1/3}$, typical of finite cylinders. The cross-over of functional behaviour occurs at the N*–H phase transition. There is therefore cylinder growth along the N* phase.

1. Introduction

Among the nucleosides commonly found in DNA and RNA, only guanosine (and some derivatives) is able to self-associate in water solution to form stable structures (reviewed in [1] and [2]): highly ordered gels, fibres and other macroaggregates have been in fact extensively investigated [3–6]. The common structural unit has been found to be a planar disc-shaped aggregate formed by four guanosine residues, hydrogen bonded in a Hoogsteen mode [7]. Furthermore, NMR investigations of 5′-guanosine monophosphate aqueous solutions showed that the self-aggregation process can also take place in very dilute solutions, via stacking of planar tetramers [8–10]. The biological relevance of this very special feature is not yet defined: on the one hand this could have had prebiotic significance in the origin of the genetic code [9–10]. On the other hand telomers and related guanine-rich sequences can form higher-order structures (quadriplexes) formed by guanine-quartet (see in particular [11]): it has been then proposed, for example, that the quadriplex formation might provide a means for homologous chromosome alignment at meiosis [12] or provide a general mechanism for aligning and pairing two duplexes for recombination ([13], see also [11]).

Recently, the aqueous solution of the dinuceoside phosphate 2′-deoxyguanylyl-(3′-5′)-2′-deoxyguanosine (d(GpG) or G2) has been studied [14, 15]. In particular, the sodium salt of G2 forms cholesteric and hexagonal liquid-crystalline phases on decreasing water content. From the analysis of the measured X-ray diffraction peaks

---

* Author for correspondence.

and optical microscopy it was suggested that the liquid-crystalline phases consist of rod-shaped chiral aggregates with negative diamagnetic anisotropy. Each chiral rod is similar to a four-stranded helix and is composed by a stacked array of planar tetramers formed by Hoogsteen bonded guanosine moieties [7], with a typical stacking distance of 3·3 Å. Further investigation on other guanosine derivatives [16, 17] also evidenced liquid-crystalline behaviour. While the overall structure of the columnar aggregates seems similar, differences were observed in the handedness of the cholesteric phase and in the concentration values at which phase transitions occur.

In this report we investigate further the structure of the cholesteric phase, N*, of G2 by X-ray diffraction in oriented samples, which allows a more defined characterization [18] of the structural unit. The isotropic phase, I, was also investigated in order to detect possible changes in the state of aggregation at the N*–I transition, which occurs [14, 15] for a concentration of 2·5 wt%.

Our data, together with those obtained on other model systems [19], might be of use in view of the recent suggestion [11–13] that the formation of guanine tetrads mediates the pairing in a parallel fashion of the four homologous chromatides during the meiosis and the dimerization of the telomeric ends of chromosomes.

2. Experimental section

The sample was prepared according to the procedure described previously [14, 15]. Aqueous solutions of different weight concentrations (1, 2, 5, 10 and 15 per cent) were conditioned in glass capillaries with 1 mm internal diameter and studied at room temperature (22 ± 1°C), since the previous study [15] has evidenced insensitivity of the results to temperature changes in the interval 5–50°C. The phase sequence is [15]

$$\mathrm{I}\ \ 2{\cdot}5\ \text{per cent}\ \ \mathrm{N}^*\ \ 18\ \text{per cent}\ \ \mathrm{H}.$$

X-ray diffraction photographs were obtained with Ni-filtered CuK$_\alpha$-radiation in a Laue transmission geometry with a very fine collimator; both the high angle and small

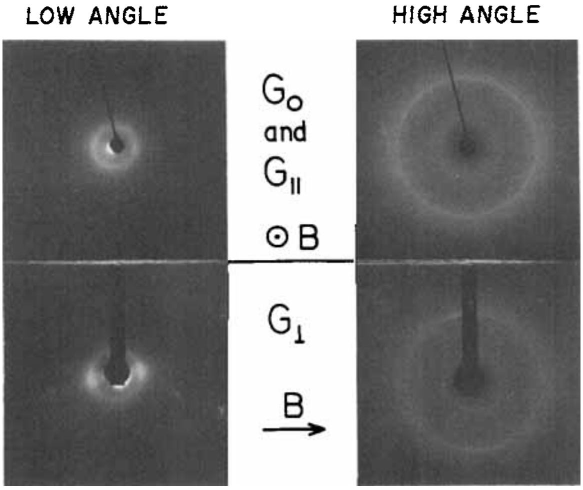

Figure 1. X-ray photographs for a sample with 15 per cent G2 in the N* phase. Results for geometries $G_\parallel$ (magnetic field **B** parallel to X-ray beam) and $G_\perp$ (**B** perpendicular to the X-ray beam) in low and high angle regions. Results for G_0 (no magnetic field) are equal to $G_\parallel$.

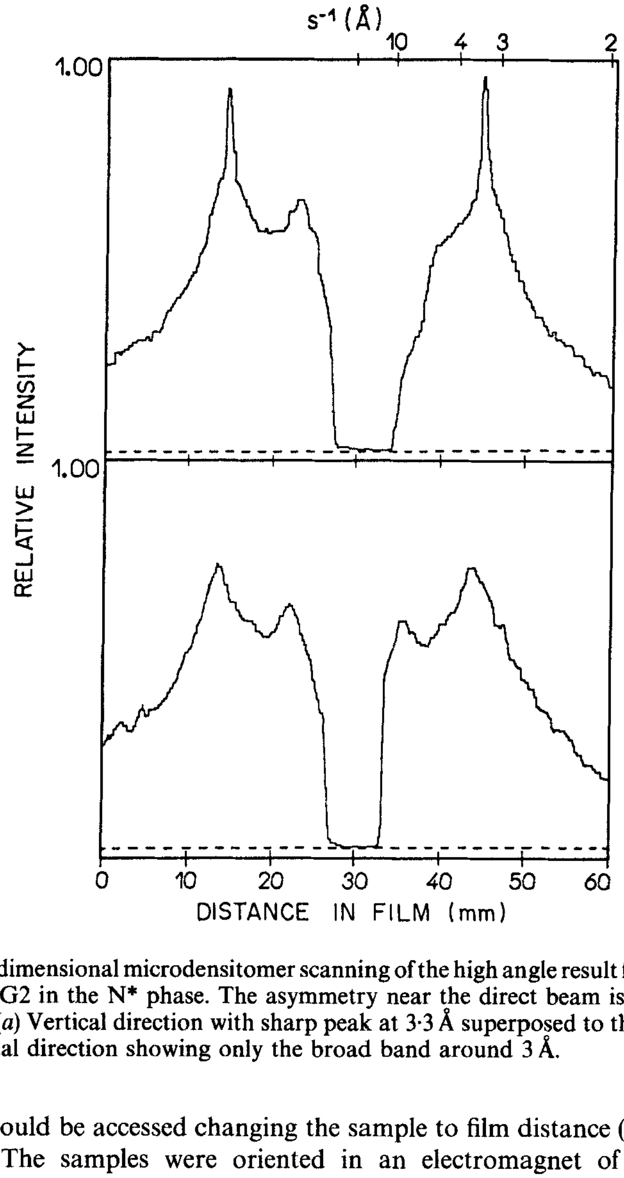

Figure 2. Unidimensional microdensitomer scanning of the high angle result for sample with 15 per cent G2 in the N* phase. The asymmetry near the direct beam is due to the beam stopper. (a) Vertical direction with sharp peak at 3·3 Å superposed to the broad band. (b) Horizontal direction showing only the broad band around 3 Å.

angle region could be accessed changing the sample to film distance (3 cm and 20 cm respectively). The samples were oriented in an electromagnet of $B = 6$ kG, perpendicular to the capillary axis, for 12 hours. Note that a permanent magnet of 4 kG resulted ineffective, even after several days. Measurements were performed in three geometries [18]: G_0 (no magnetic field), $G_\perp$ (X-ray beam perpendicular to **B** direction) and $G_\parallel$ (X-ray beam parallel to **B** direction). The systematics of measurement was $G_0 \rightarrow G_\perp \rightarrow G_\parallel \rightarrow G_\perp$ to assure the permanence of residual orientation after removal of the field. A microdensitometer was used for quantitative analysis of the photographs.

3. Results

Figure 1 shows results for a 15 wt% sample at small angle SA and high angle HA in the three geometries G_0, $G_\parallel$ and $G_\perp$. In the SA region a single diffraction is present in the cholesteric phase; this peak was not accurately investigated in previous work [15–17], since its detection requires special collimation. In the HA region there is a sharp peak,

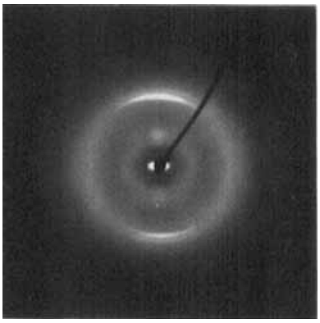

Figure 3. X-ray photograph for a sample in N* phase near the H–N* transition, showing in vertical direction the 3·3 Å peak as well as the 7 Å band in the high angle region. The low angle region has an equatorial peak at $s^{-1}=65$ Å.

corresponding to a spacing of (3·3 ± 0·1) Å, interpreted [15] as the distance between the tetrameric discs. This sharp peak (present in N* and H phases) is superposed to a broad band, since both water and the empty capillary have bands in this region (centred at 3·1 Å for water and 3·5 Å for the glass capillary). Figure 2 shows microdensitometer records of HA results, evidencing the profile of the sharp peak superposed to the broad band in one direction.

There is also a band in the 7 Å region, of more difficult analysis: pure water has a band at 7 Å, but the band appears partially oriented in oriented N* phases, evidencing a diffraction due to *G*2. Figure 3 shows a photograph obtained with a N* sample very near the N*–H transition, where the oriented band at 7 Å can be clearly seen. This diffraction has not been reported in previous work [15–17] and will be discussed later on. In this sample a weak peak at 3·1 Å seems also to be present, besides the strong peak at 3·3 A°.

Changing concentration in the N* phase (10 and 5 wt% of *G*2) leads to a change only in the peak position of the low angle region. The high angle diffraction and the symmetry of all results in the oriented samples remained the same within the N* phase.

G_0 results showed, no surface orientation, which is characteristic of micellar nematic phases [18]; therefore no compromise between surface and magnetic orientation should be expected.

Optical microscopy results [14, 15] evidence in N* phase negative diamagnetic anisotropy ($\Delta\chi < 0, \mathbf{n} \perp \mathbf{B}$). Since results for G_0 and $G_{\parallel}$ are equal, the director rotates in the plane perpendicular to **B**. Results for $G_{\perp}$ show that the sharp peak at 3·3 Å refers to a characteristic distance along the **n** direction, while the band at SA refers to a characteristic distance perpendicular to **n** director and along the **B** direction. This gives full support to the previously proposed model [15]: a stacking of tetrameric discs, with **n** perpendicular to the discs, or **B** in the disc plane. The SA reflects the diffraction due to neighbouring stacking of discs, or cylinders with **n** parallel to the cylinder axis.

It should be stressed that in the N* phase the cylinders are not strictly parallel, but twisted in a helical structure, with **n** rotating in the plane perpendicular to **B**. In the hexagonal phase the twist is destroyed and cylinders become parallel. The twist requires more free space, what is possible only in a less concentrated solution.

In the I phase (1 and 2 wt% of G2) results are indistinguishable from water: the two broad bands are present in HA, but the sharp peak is absent, and no SA peak appears, possibly due to low intensities.

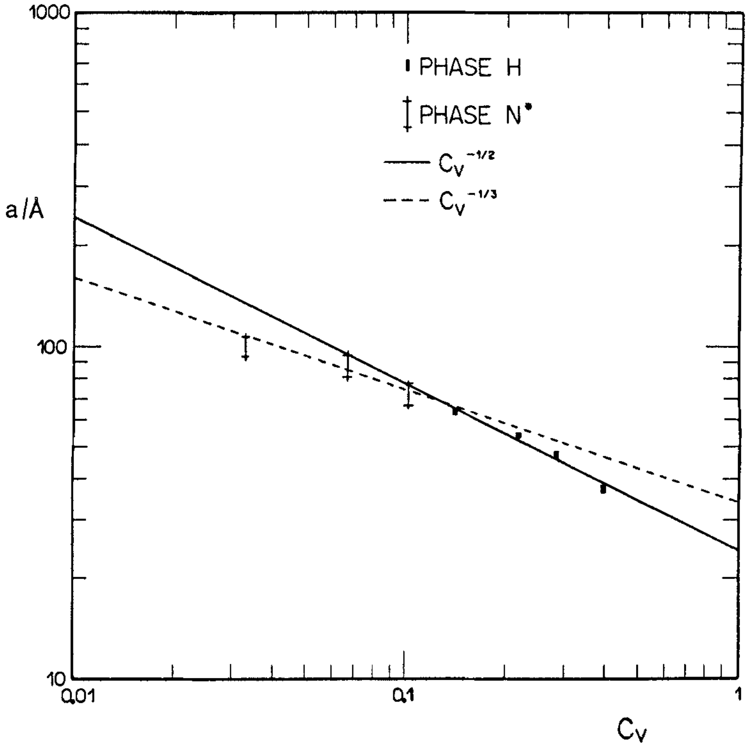

Figure 4. Distance between cylinders a as a function of the G2 volume concentration c_v. Points for the H phase include experimental errors. For the N* phase the upper limit corresponds to $a=(2/\sqrt{3})s^{-1}$ and the lower limit to $a=s^{-1}$. Also shown are the curves for infinite ($c_v^{-1/2}$) and finite ($c_v^{-1/3}$) cylinders.

Figure 4 shows the structural parameter a obtained from the position of the low angle peak as a function of c_v, the G2 volume concentration (calculated by using the value of 0·651 cm^3/g as specific volume) [20] compared with previous results [15] in the H phase. The average distance a between cylinders is estimated in the N* phase to be within the limits $a=s^{-1}$ and $a=(2/\sqrt{3})s^{-1}$ (as it would be for $d_{100}=s^{-1}$, with local hexagonal order).

It has been shown theoretically [21–23] that the exponents $-1/2$ and $-1/3$ for the c_v dependence of interparticle distance are the fingerprints of respectively infinite objects (with interparticle distance decreasing in a plane) and finite objects (with volume around particles decreasing in all three dimensions). Our results show clearly a cross-over behaviour between finite and infinite objects near the H–N* transition.

It should be stressed that recent results in the H phase in the system sodium dodecyl sulphate/water [23] gave a $c_v^{-1/3}$ dependence in the H range, after a H–I direct transition.

It has been predicted theoretically [22] that the direct H–I transition is expected in the case of a polydisperse system of concentrated and small spherocylinders, while the H–N–I transition sequence is expected for more diluted and longer cylinders.

Our results show that the H–N* transition in this system occurs for infinite cylinders.

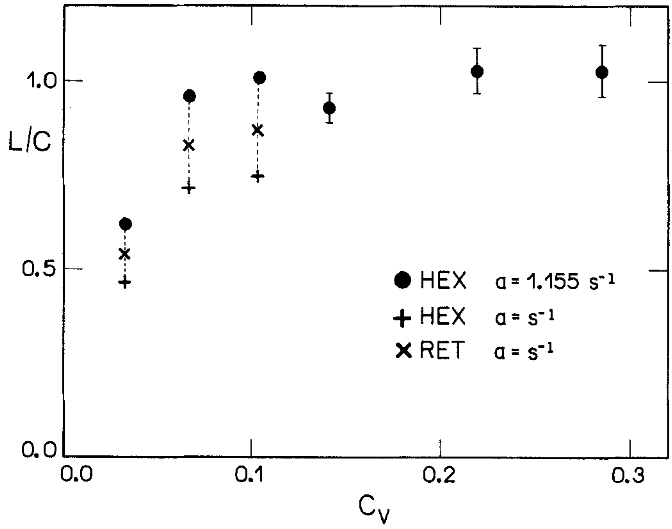

Figure 5. Ratio between cylinder length L and cell height C as a function of the G2 volume concentration c_v. Results obtained from equation (1) for local hexagonal order and from equation (3) for local rectangular order.

Let us analyse results from figure 4 supposing [23] an hexagonal cell of height C and a cylindrical micelle with radius R and length L. The amphiphile/water volume ratio must be the same in the unit cell as in the whole sample. Therefore

$$(L/C)R^2=(\sqrt{3}/2\pi)c_v a^2. \tag{1}$$

For infinite cylinders ($L=C$) with constant R one should have

$$a=(2\pi/\sqrt{3})^{1/2}Rc_v^{-1/2} \tag{2}$$

Figure 4 shows a good adjustment to the data in the H phase obtained with $R=12{\cdot}8$ Å, a reasonable value for G2 from chemical data [15–17, 24].

In the N* phase, infinite cylinders correspond to the assignment $s^{-1}=d_{100}$ for higher concentrations. However a deviation from infinite cylinders occurs clearly for smaller concentrations, near the N*–I transition. With the assignment $s^{-1}=a$, the deviation occurs in the whole N* range.

Figure 5 gives L/C values obtained from equation (1). In the N* phase, besides the previous assignments for a in a local hexagonal order ($a=s^{-1}$ and $a=1{\cdot}155\,s^{-1}$), the assignment for a rectangular ($s^{-1}=a$) local order is also shown, corresponding to

$$L/C=(a^2/\pi R^2)c_v. \tag{3}$$

Even considering that part of the excess water could be taken by the twist of the N* phase, there are clear indications of finite cylinders in the less concentrated N* phase, with a $c_v^{-1/3}$ behaviour.

This result, together with sizes estimated from neutron small angle scattering in the isotropic phase (69·2 Å at 1 wt% and 71·2 Å at 1·5 wt%) [25] indicates that cylinders are growing along the N* phase.

Let us now discuss the origin of the band at (7·0 ± 1) Å, which is oriented in the same direction as the 3·3 Å sharp peak. One could try to associate the 7 Å diffraction to the helix structure internal to the chiral cylinders, that correlates with disc rotation around n [16]. Since the typical cross diffraction of a helix is not seen, the 7 Å band could only be understood in terms of the 'coiled coil' hypothesis [26, 27], corresponding to a compound helix (small pitch and large pitch helices in the same structural unit). Another possibility would be to ascribe it to the presence of partial order in the position of the Na counter ions that contribute to the aggregation of the discs. The Na counter ions would be present every two discs, or between the pseudo-octamers proposed in [15].

4. Conclusion

The rod structure previously proposed [15] is confirmed by the symmetry of the diffraction in oriented samples. The analysis of the distance *a* between rods with concentration shows a functional change in phases N* and H, corresponding to finite cylinders in phase N*, growing to infinite in phase H.

We would like to thank CNR (Italy) and CNPq (Brazil) for financial support as well as FAPESP for a fellowship (R. Itri). Dr. G. P. Spada introduced the study of (dGpG) and Dr. A. Garbesi provided the G2 sample. The technical assistance of D. Bulla and S. A. Silva is acknowledged.

References

[1] Saenger, W., 1984, *Principles of Nucleic Acids Structure* (Springer), pp. 315–320.
[2] Sundquist, W. I., 1991, *Nucleic Acids in Molecular Biology*, edited by D. M. Lilley and F. Eckstein (Springer), Vol. 5.
[3] Gellert, M., Lipsett, M. N., and Davies, D. R., 1962, *Proc. natn. Acad. Sci. U.S.A.*, **48,** 2013.
[4] Tougard, P., Chantot, J. F., and Guschlbauer, W., 1973, *Biochim. biophys. Acta*, **308,** 9.
[5] Zimmermann, S. B., Cohen, G. H., and Davies, D. R., 1975, *J. molec. Biol.*, **92,** 181.
[6] Zimmermann, S. B., 1976, *J. molec. Biol.*, **106,** 663.
[7] Hoogsten, K., 1959, *Acta crystallogr.*, **12,** 822.
[8] Pinnavaia, T. J., Marshall, C. L., Mettler, C. M., Fisk, C. L., Miles, F. T., and Becker, E. D., 1978, *J. Am. chem. Soc.*, **100,** 3625.
[9] Borzo, M., Detellier, C., Laszlo, P., and Paris, A., 1980, *J. Am. chem. Soc.*, **102,** 1124.
[10] Detellier, C., and Laszlo, P., 1980, *J. Am. chem. Soc.*, **102,** 1135.
[11] Sen, D., and Gilbert, W., 1991, *Curr. Opin. struct. Biology*, **1,** 435.
[12] Sen, D., and Gilbert, W., 1988, *Nature, Lond.*, **334,** 364; 1990, *Ibid.*, **344,** 410.
[13] Sundquist, R. I., and Klug, A., 1989, *Nature, Lond.*, **342,** 825.
[14] Spada, G. P., Carcuro, A., Colonna, F. P., Garbesi, A., and Gottareli, G., 1988, *Liq. Crystals*, **3,** 651.
[15] Mariani, P., Mazabard, C., Garbesi, A., and Spada, G. P., 1989, *J. Am. chem. Soc.*, **111,** 6369.
[16] Bonazzi, S., Capobianco, M., Morais, M. M. de, Garbesi, A., Gottarelli, G., Mariani, P., Borsi, M. G. P., Spada, G. P., and Tondelli, L., 1991, *J. Am. chem. Soc.*, **113,** 5809.
[17] Bonazzi, S., Morais, M. M. de, Garbesi, A., Gotarelli, G., Mariani, P., and Spada, G. P., 1991, *Liq. Crystals*, **10,** 495.
[18] Amaral, L. Q., 1989, *J. appl. Crystallogr.*, **22,** 519.
[19] Jin, R., Breslauer, K. J., Jones, R. A., and Gaffney, B. L., 1990, *Science, N.Y.*, **250,** 543.
[20] Iball, J., Morgan, C. H., and Wilson, H. R., 1963, *Nature, Lond.*, **199,** 688.
[21] Hentschke, R., Taylor, M. P., and Herzfeld, J., 1989, *Phys. Rev.* A, **40,** 1678; 1989, *Phys. Rev. Lett.*, **62,** 800.
[22] Hentschke, R., and Herzfeld, J., 1991, *Phys. Rev.* A, **44,** 1148.
[23] Amaral, L. Q., Gulik, A., Itri, R., and Mariani, P., 1992, *Phys. Rev.* A (in the press).
[24] Fisk, C. L., Becker, E. D., Miles, H. T., and Pinnavaia, T. P., 1982, *J. Am. chem. Soc.*, **104,** 3307.
[25] Carsughi, F., Ceretti, M., and Mariani, P., *Europ. Biophys. J.* (in the press).
[26] Crick, F. H. C., 1953, *Acta crystallogr.*, **6,** 685; 689; 1952, *Nature, Lond.*, **170,** 882.
[27] Pauling, L., and Corey, R. B., 1953, *Nature, Lond.*, **171,** 59.